Comparative experiments regarding approaches to feedforward hysteresis compensation for piezoceramic actuators

2014 Smart Mater. Struct. 23 095029

(http://iopscience.iop.org/0964-1726/23/9/095029)

IOP Publishing Smart Materials and Structures
Smart Mater. Struct. **23** (2014) 095029 (11pp) doi:10.1088/0964-1726/23/9/095029

Comparative experiments regarding approaches to feedforward hysteresis compensation for piezoceramic actuators

Guo-Ying Gu and Li-Min Zhu

State Key Laboratory of Mechanical System and Vibration, School of Mechanical Engineering, Shanghai Jiao Tong University, 200240, People's Republic of China

E-mail: guguoying@sjtu.edu.cn

Received 13 April 2014, revised 13 June 2014
Accepted for publication 7 July 2014
Published 14 August 2014

Abstract

Piezoceramic actuators (PCAs) are desired devices in many micro/nano-positioning applications. The performance of PCA-based applications is severely limited by the presence of hysteresis nonlinearity. To remedy the hysteresis nonlinearity in such systems, feedforward hysteresis compensation is the most common technique. In the literature, many different feedforward hysteresis compensation approaches have been developed, but there are no comparative studies of these approaches. Focusing on the modified Prandtl-Ishlinskii model (MPIM) for asymmetric hysteresis description of piezoceramic actuators, three feedforward hysteresis compensation approaches—inverse hysteresis compensation (IHC), without inverse hysteresis compensation (WIHC), and direct inverse hysteresis compensation (DIHC)—are developed and compared in this paper. Extensive comparative experiments were conducted on a PCA-actuated stage to verify the effectiveness of the three different feedforward control approaches to hysteresis compensation. The experimental results show that the performances among the three approaches are rather similar, and the main differences among them are due to the specific implementation of each approach.

Keywords: piezoceramic actuator, asymmetric hysteresis, feedforward hysteresis compensation

1. Introduction

Nowadays, piezoceramic actuators (PCAs) are being applied more and more increasingly in many micro-positioning systems such as micro/nano-manipulations [1–3] and scanning probe microscopies [4–6]. The benefit of selecting PCAs in these applications lies in the fact that PCAs directly transform electrical signals into mechanical signals for managing small displacements in the range of tens of pm (1 pm = 10^{-12} m) to several hundreds of μm based on the converse piezoelectric effect [7]. They have attractive advantages of fast frequency response, nanometer scale resolution, and high stiffness. However, the accuracy of PCAs is highly limited by the inherent hysteresis nonlinearity of the piezoceramic materials, which is a consequence of the effects of domain switching in the piezoceramic materials due to the action of the applied electric field. Hysteresis is a kind of a multi-valued nonlinearity with nonlocal memory [8, 9], which means the displacement of the PCAs depends not only on the current input voltage but also on its history. Therefore, development of control approaches to remedy the hysteresis is a challenging task.

To tackle this challenge, many control efforts have been made over the last decade. Roughly speaking, the existing control techniques can be classified into the following three categories: i) charge control, ii) feedback voltage control, and iii) feedforward voltage control. The main benefit of using charge control is the reduction of hysteresis between the displacement and the applied charge. Experiments indicate that hysteresis can be reduced at least to one-fifth compared with voltage control [10, 11]. The disadvantage of charge control is the requirement of additional electric circuits or devices, which increases the complexity and cost of the control hardware. Feedback voltage control is the second technique to eliminate the hysteresis of PCAs. In recent years, many feedback control schemes based on modern control

techniques have been proposed for high-precision tracking control of PCAs, including, for instance, state feedback control [12], optimum linear quadratic Gaussian control [5], H_∞ control [13], quantitative feedback control [14], sliding mode control [15], robust adaptive control [16], and fuzzy control [17]. In this category, the hysteresis is generally treated as disturbances, and the main difficulty lies in the stability analysis of the entire closed-loop system. In the voltage control case, the third technique is to develop a feedforward compensator with a well-defined hysteresis model [8, 18–24]. As of today, feedforward voltage control is the most commonly adopted control technique to compensate for the hysteresis nonlinearity of PCAs. In this work, we focus mainly on reviewing and comparing the approaches using the third technique for hysteresis compensation.

The key to the feedforward control technique is to find an available hysteresis model that can precisely describe hysteresis behaviors. Many popular mathematical models have been developed, such as the Jiles-Atherton model, Duhem model, Bouc-Wen model, Preisach model, and Prandtle-Ishlinskii model. With a developed hysteresis model, the subsequent step is to construct a feedforward controller for hysteresis compensation. A review of the literature reveals that, there are three approaches to accomplishing this purpose. i) Inverse hysteresis compensation approach: a hysteresis model is used to describe the hysteresis of PCAs and an inverse model of the hysteresis model is then constructed to cancel the hysteresis nonlinearity [8, 9, 19, 25–32]. ii) Without inverse hysteresis compensation approach: a hysteresis model is adopted to describe the hysteresis of PCAs and is used directly for hysteresis compensation without inverse model construction [24, 33–35]. iii) Direct inverse hysteresis compensation approach: a hysteresis model is directly utilized to describe the inverse hysteresis of PCAs for hysteresis compensation [20, 23, 36, 37]. This approach also avoids the construction of an inverse model for the adopted hysteresis model.

As can be seen from the preceding discussion, hysteresis compensation of PCAs is an interesting topic, and many researchers devote themselves to this field. However, until now, no comparative study of the different feedforward approaches has been undertaken. The development of this work is a continuation of the authors' work presented in [9]. The previous work was limited to developing the novel modified Prandtl-Ishlinskii model (MPIM). Therefore, it did not provide insight into comparisons of different feedforward hysteresis compensation approaches.

Focusing on the MPIM for asymmetric hysteresis description of a piezoelectric actuator, the motivation of this paper is to develop and compare the three feedforward hysteresis compensation techniques for PCAs, where the hysteresis is described by the MPIM. The principles and implementation steps of the three feedforward control approaches for hysteresis compensation are presented first in this work. Then comparative experiments are conducted in real time to evaluate and compare their hysteresis compensation performances.

The contributions of this paper are as follows: i) A novel feedforward hysteresis compensator with the MPIM is proposed using the without inverse hysteresis compensation approach; ii) the characteristics and performances of the three hysteresis compensation approaches are discussed and evaluated for asymmetric hysteresis compensation of PCAs. We note that feedforward approaches have been reported for hysteresis compensation of the PCAs and have proved to be useful for performance improvement, but a comparative study of different feedforward approaches has not been reported before. Our experimental results demonstrate that the performances among the three approaches are rather similar, and the main differences among them are due to the specific implementation of each approach. These results may also show why so many researchers try to develop different hysteresis compensators with different hysteresis models according to their applications.

The remainder of this paper is organized as follows. Section 2 briefly introduces the MPIM used in this work. Section 3 presents three feedforward contol approaches for hysteresis compensation. In section 4, a PCA-based experimental platform is built and comparative experiments are conducted. Section 5 concludes this paper.

2. Modified Prandtl-Ishlinskii model

The Prandtl-Ishlinskii model (PIM) is a famous operator-based phenomenological model to describe hysteresis nonlinearity having the advantage of the existence of the analytical inverse. The classical PIM is effective for symmetric hysteresis description. However, it is insufficient to describe asymmetric hysteresis. As an extension, a modified Prandtl-Ishlinskii model (MPIM) [9] defined by weighted one-sided play operators and a polynomial input function is developed to describe the asymmetric hysteresis of PCAs. Before presenting the different feedforward control approaches, a brief introduction of the MPIM is given in this section.

2.1. Play operator

The play operator is the basic hysteresis operator with symmetric and rate-independent properties. The one-dimensional play operator can be recognized as a piston with a plunger of length $2r$. The output $F_r[x](t)$ is the position of the center of the piston, and the input x is the plunger position. Considering the positive excitation nature of the used piezoceramic actuator, a one-sided play operator with $r \geqslant 0$ is given as follows [9]:

$$F_r[x](0) = f_r(x(0), 0)$$
$$F_r[x](t) = f_r\left(x(t), F_r[x](t_i)\right) \tag{1}$$

for $t_i < t \leqslant t_{i+1}$, $0 \leqslant i \leqslant N-1$ with

$$f_r(v, w) = \max(v - r, \min(v, w)) \tag{2}$$

where $0 = t_0 < t_1 < \ldots < t_N = t_E$ is a partition of $[0, t_E]$, such that the function $x(t)$ is monotone on each of the

subintervals $[t_i, t_{i+1}]$. The argument of the operator $F_r[x]$ is written in square brackets to indicate functional dependence because it maps a function to another function.

2.2. MPIM

On the basis of the one-sided play operator (1), the MPIM is expressed as [9]

$$y(t) = g(x(t)) + \int_0^R p(r)F_r[x](t)dr \tag{3}$$

where $g(x(t)) = a_1x^3(t) + a_2x(t)$ is a polynomial input function with constants a_1 and a_2, and $p(r)$ is a density function that can be obtained by the experimental data. The density function $p(r)$ generally vanishes for large values of r, whereas the choice of $R = \infty$ as the upper limit of integration is widely used in the literature for the sake of convenience.

For implementation of the real-time feedforward compensator, the MPIM (3) is approximated by the discrete form as follows:

$$y(t) = g(x(t)) + \sum_{i=1}^{n} b(r_i)F_{r_i}[x](t) \tag{4}$$

where n is the number of the adopted play operators for modeling, and $b(r_i) = p(r_i)(r_i - r_{i-1})$ is the weighted coefficient for the threshold r_i.

3. Feedforward hysteresis compensation approaches

The nature of feedforward hysteresis compensation approaches is to develop feedforward controllers in series for a real hysteretic system. In this scheme, the developed feedforward controllers can represent the inverse hysteresis behaviors of PCAs. Therefore, hysteresis can be compensated by the feedforward controller as illustrated in figure 1, where $y_d(t)$, $v(t)$, and $y(t)$ are the desired position, control action, and actual position of the PCA, respectively. In this section, three feedforward hysteresis compensation approaches are presented and discussed together with the MPIM.

3.1. Inverse hysteresis compensation

Inverse hysteresis compensation (IHC) is a four-step approach. The first step is hysteresis modeling, which adopts a hysteresis model to describe the hysteresis of a PCA. The second step is parameter identification, or identifying the parameters of the adopted model. The third is inverse construction, or developing an inverse model of the identified hysteresis model. The fourth step is controller design, where the constructed inverse is used in the feedforward path for hysteresis compensation. As an illustration, figure 2(a) shows the implementation steps of the IHC approach.

From figure 2(a), it can be seen that the key to the IHC approach is to construct an inverse model of the adopted hysteresis model. With the MPMI model for hysteresis description (4), the inverse model of the MPIM can be derived by the implicit operator equation [9]

$$v(t) = P_1^{-1}[w](t) \tag{5}$$

for the inverse compensator

$$v(t) = P^{-1}[y_d](t) \tag{6}$$

where $w = y - P_c[v]$, $P_c[v](t) = a_1v^3(t)$ is a new model component, and P_1^{-1} is expressed as

$$P_1^{-1}[w](t) = \hat{a}_2w(t) + \sum_{j=1}^{n} \hat{b}_j F_{\hat{r}_j}[w](t) \tag{7}$$

with

$$\hat{r}_j = a_2r_j + \sum_{i=1}^{j-1} b_i(r_j - r_i)$$

$$\hat{a}_2 = \frac{1}{a_2}$$

$$\hat{b}_j = -\frac{b_j}{\left(a_2 + \sum_{i=1}^{j-1} b_i\right)\left(a_2 + \sum_{i=1}^{j} b_i\right)}$$

In accordance with (5)–(8), a block diagram of the feedforward controller using the IHC approach is depicted in figure 3.

3.2. Without inverse hysteresis compensation

The second feedforward control approach is considered an approach without inverse hysteresis compensation (WIHC), which means that one does not need to construct an inverse model of the adopted hysteresis model in the feedforward controller. Figure 2(b) shows the steps of the WIHC approach, which is a three-step approach. The first step is hysteresis modeling, which adopts a hysteresis model to describe the hysteresis of a PCA. The second step is parameter identification, or identifying the parameters of the adopted model. The third step is controller design directly using the identified hysteresis model, which is different from the IHC approach that uses the inverse model for controller design. Note that the first and second steps of the WIHC are same as those for the IHC. Comparing figure 2(a) with figure 2(b), the WIHC avoids construction of the inverse model.

The key idea of the WIHC approach is to directly use the adopted hysteresis models to develop the hysteresis compensators with the multiplicative structure. In [33], the feedforward controller with the Bouc-Wen model was first developed to compensate for the hysteresis of PCAs based on the multiplicative structure. Subsequently, Li *et al* [24] extended the multiplicative structure with the Preisach model for hysteresis compensation. As a continuation, this paper intends to develop a novel multiplicative structure–based hysteresis compensator with the MPIM as feedforward. In this way, the control law v of the feedforward compensator using the WIHC approach can be extracted from the discrete MPIM

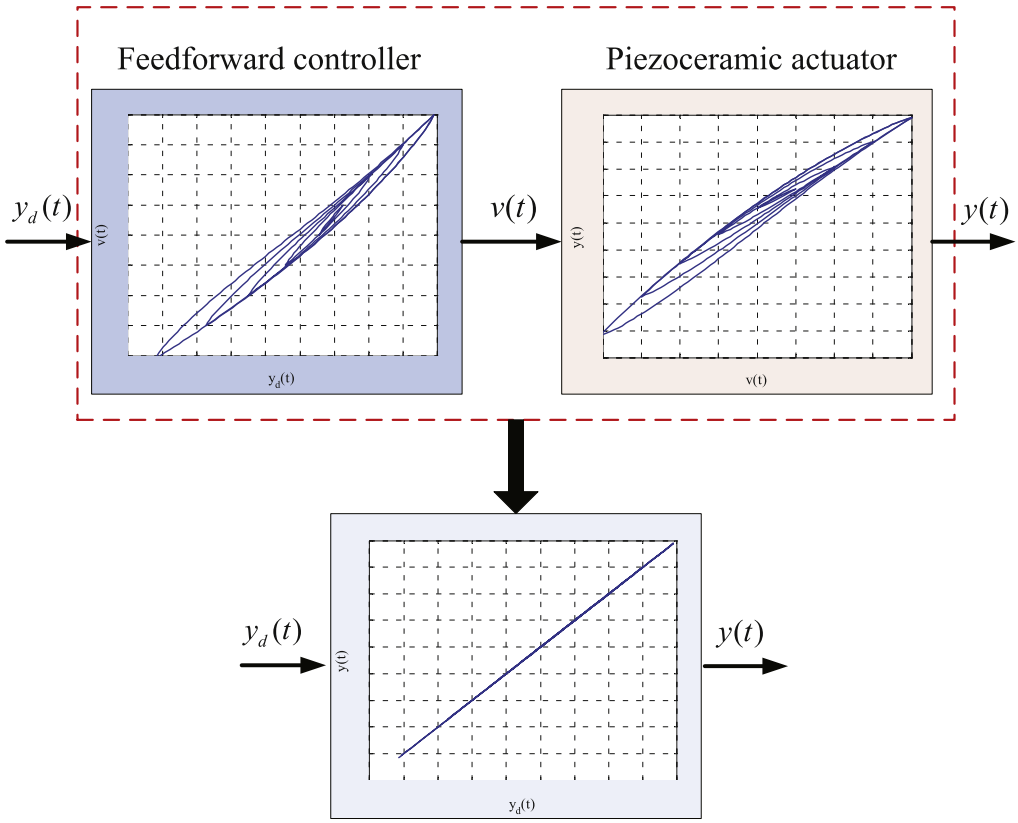

Figure 1. Block diagram of the feedforward controller for hysteresis compensation.

(4) as

$$v(t) = \frac{1}{a_2}\left(y_d(t) - H[v](t)\right) \tag{9}$$

where $H[v](t) = a_1 v^3(t) + \sum_{i=1}^{n} b(r_i) F_{r_i}[v](t)$.

It can be seen from (9) that the MPIM is used directly to develop the feedforward controller without constructing the inverse. The block diagram of the WIHC approach is shown in figure 4.

3.3. Direct inverse hysteresis compensation

Direct inverse hysteresis compensation (DIHC) is a three-step approach as well and is illustrated in figure 2(c). Rather than model the hysteresis effect of the PCA, the first step of the DIHC approach is to directly model the inverse hysteresis effect of the PCA, which is different from the IHC and WIHC approaches. The new concept in the DIHC approach is motivated by the fact that the inversion of the hysteresis effect is by nature hysteresis loops that can be described by a hysteresis model [20, 23, 36]. The second step is parameter identification, which identifies the parameters of the MPIM. The third step is controller design using the identified inverse hysteresis model. Therefore, the DIHC approach also avoids the construction of the inverse mathematical model.

Based on the principle of the DIHC approach, the feedforward controller can be directly developed by the identified MPIM [20]:

$$v(t) = P[y_d](t) = a_1 y_d^3(t) + a_1 y_d(t) + \sum_{i=1}^{n} b(r_i) F_{r_i}[y_d](t) \tag{10}$$

The block diagram of the DIHC is shown in figure 5(a).

4. Experiments

In this section, a PCA-based experimental platform is built and comparative experiments are conducted to evaluate and compare the hysteresis compensation performances of the IHC, WIHC, and DIHC approaches.

4.1. Experimental setup

The experimental platform is shown in figure 6. It consists of a host computer, a dSPACE-DS1103 controller board, a piezoceramic actuator, a piezoelectric amplifier, a strain gauge position sensor, and a sensor signal conditioner. The host computer provides a user interface for the dSPACE-DS1103 controller board. The dSPACE-DS1103 controller board equipped with 16-bit DACs and 16-bit ADCs is adopted to generate control codes and obtain the displacement information. The adopted PCA is a preloaded piezoceramic stack actuator (PSt 150/7/100 VS12 from Piezomechanik in Germany), which is used to drive the one-dimensional flexure

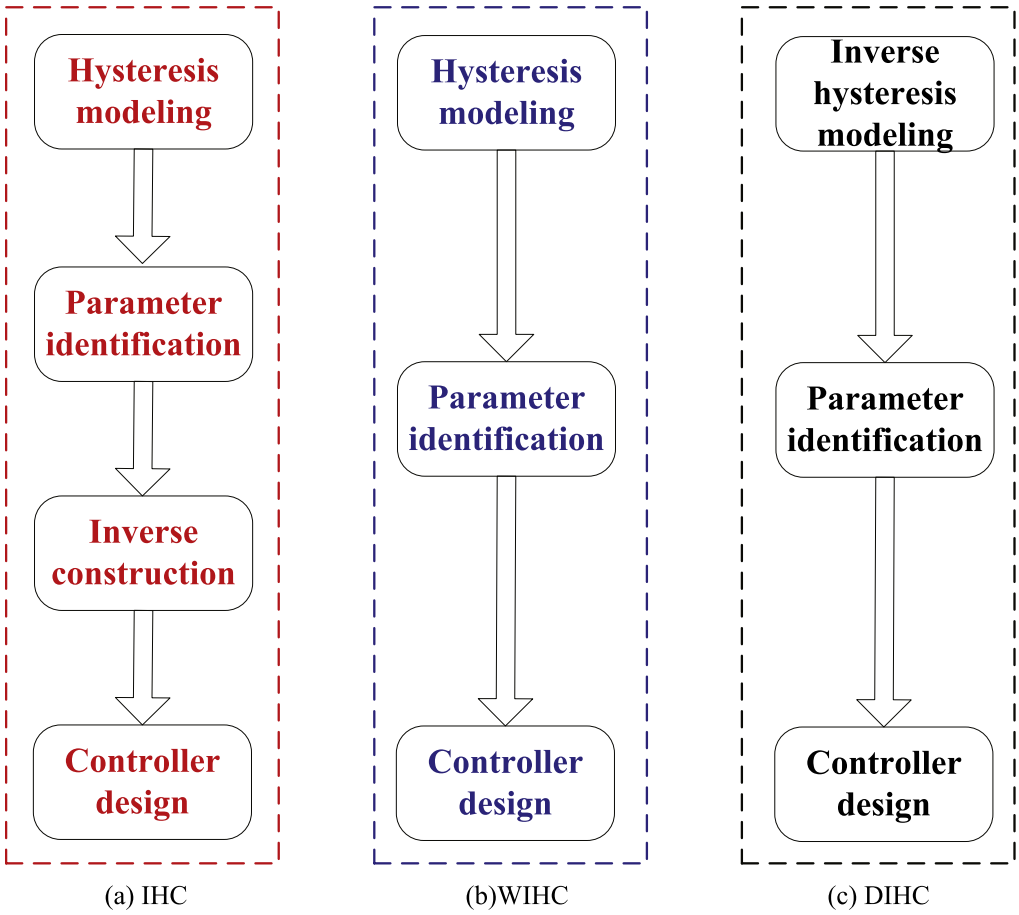

Figure 2. Implementation steps of three feedforward hysteresis compensation approaches.

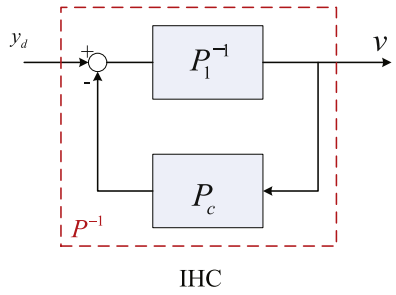

Figure 3. Block diagram of the feedforward controller using the IHC approach.

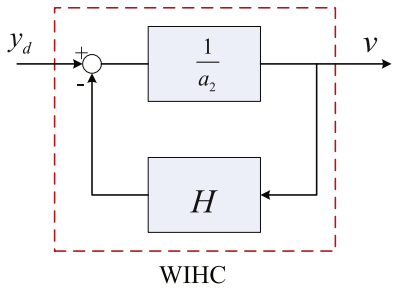

Figure 4. Block diagram of the feedforward controller using the WIHC approach.

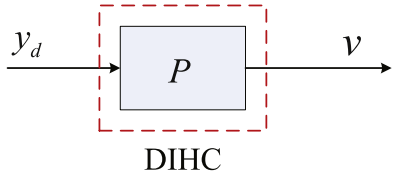

Figure 5. Block diagram of the feedforward controller using the DIHC approach.

hinge guiding stage (FHGS) with the nominal 75-μm displacement. The piezoelectric amplifier (PEA) has a fixed gain of 15 that provides excitation voltage for the PCA in the 0–150 V range. In the PCA, the strain gauge sensor (SGS) is bonded to measure the real-time position of the PCA. The SGS is a contact-type sensor that can offer high resolution and bandwidth [38]. The output signals of the SGS are adjusted by the signal conditioner (SC) and then sampled by the 16-bit ADC of the dSPACE-DS1103 control board. As an illustration, figure 6(b) shows a block diagram of the experimental platform.

4.2. Parameter identification

To experimentally compare the different feedforward approaches, the parameters of the MPIM should be identified first. As addressed in section 3, the IHC and WIHC utilize the MPIM to describe the hysteresis of the tested PCA, whereas

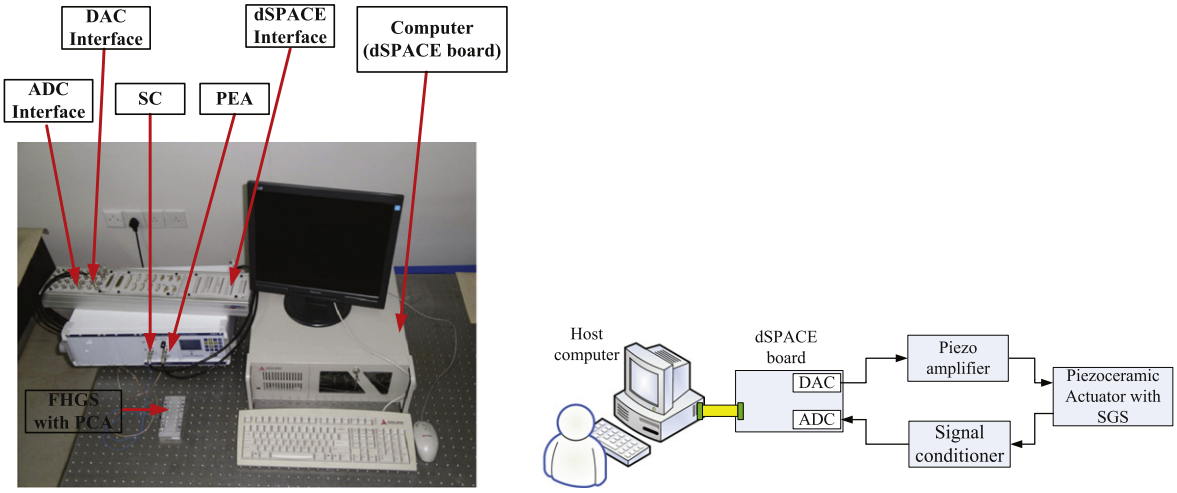

(a) Experimental platform (b) Block diagram

Figure 6. Experimental setup.

Table 1. Identified parameters of the MPIM for the IHC and WIHC approaches. The definitions of the parameters are given under (3).

Number	r_i	b_i	a_i
1	0	0.2313	−0.1569
2	0.1	0.3059	0.4603
3	0.2	0.0155	
4	0.3	0.0752	
5	0.4	0.0683	
6	0.5	0.0252	
7	0.6	0.0035	
8	0.7	0.0094	
9	0.8	0.0264	
10	0.9	0.0032	

Table 2. Identified parameters of the MPIM for the DIHC approach. The definitions of the parameters are given under (3).

Number	r_i	b_i	a_i
1	0	−0.00002	0.1608
2	0.1	−0.26603	1.2588
3	0.2	−0.10684	
4	0.3	−0.01221	
5	0.4	−0.08412	
6	0.5	−0.00238	
7	0.6	−0.00328	
8	0.7	−0.01115	
9	0.8	−0.03417	
10	0.9	−0.47999	

the DIHC adopts the MPIM to represent the inverse hysteresis of the PCA. Therefore, the parameters of the MPIM in the IHC and WIHC approaches are the same.

Many identification algorithms such as the least-squares method, fuzzy algorithms, and particle swarm optimization (PSO) have been proposed to identify the hysteresis models [8, 39, 40]. In [39], PSO has been shown to be superior to its competitors for identification of the P-I model. Therefore, the PSO algorithm is used in this work to identify the model parameters. In practice, the threshold values r_i in the MPIM are given by

$$r_i = \frac{i-1}{n}\|x(t)\|_\infty, \quad i = 1, 2, ..., n \tag{11}$$

where $x(t)$ is the input of the MPIM model, $\|x(t)\|_\infty = 1$ in the normalized case, and $n = 10$ is chosen in this study. It should be noted that in the IHC and WIHC approaches, $x(t)$ represents the control input $v(t)$, whereas in the DIHC approach $x(t)$ represents the desired trajectory $y_d(t)$. Table 1 lists the identified parameters of the MPIM for the IHC and WIHC approaches. Table 2 lists the identified parameters of the MPIM for the DIHC approach.

4.3. Comparative study

In this comparative study, a desired trajectory $y_d(t) = 37.35 + 10.5\sin(\pi t + 2.6) + 10.5\sin(1.6\pi t + 3) + 15.75\sin(2\pi t + 1.5)$ (μm) is adopted to evaluate the performances of the three hysteresis compensation approaches.

To quantify the performances of different feedforward control approaches, the following indexes are used.

(D1) $e_m = \frac{\max(|y(t) - y_d(t)|)}{\max(y_d(t)) - \min(y_d(t))} \times 100\%$: the maximum value of the tracking error.

(D2) $e_{rms} = \frac{\sqrt{(1/T)\int_0^T (y(t) - y_d(t))^2 dt}}{\max(y_d(t)) - \min(y_d(t))} \times 100\%$: the root mean square value of the tracking error and T represents the total running time.

4.3.1. Tests without hysteresis compensation. Before comparing the hysteresis compensation performances of different control approaches, the hysteresis nonlinearity of the adopted PCA should be given. figure 7 shows the experimental results with a feedforward gain component. It

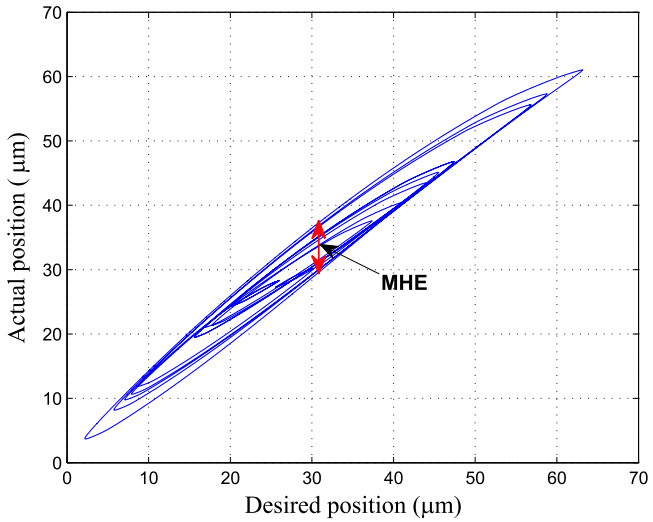

Figure 7. Hysteresis nonlinearity of the tested PCA.

can be seen that the hysteresis is the complex nonlinearity with multi-valuedness and nonlocal memory. We can determine that the maximum hysteresis caused error is about $e_{mhe} = 13\%$, defined as

$$e_{mhe} = \max \left| \frac{MHE}{\max(y_d) - \min(y_d)} \right| \times 100\%. \quad (12)$$

Therefore, it is necessary to develop control approaches to remedy the hysteresis nonlinearity.

4.3.2. IHC. With the IHC approach, figure 8 shows the trajectory-tracking results. The map of the desired position and actual position is shown in figure 8(a). It can be determined that the IHC approach reduces the hysteresis e_{mhe} from 13% to less than 3%. With the IHC, figure 8(b) shows the trajectory tracking response. It can be seen that the response of the PCA follows the desired trajectory well. In addition, the tracking error is shown in figure 8(c), where e_m and e_{rms} are 2.66% and 0.75%, respectively.

4.3.3. WIHC. In this section, the experimental results with the WIHC approach are shown in figure 9. Figure 9(a) shows the map of the desired position and actual position, where the hysteresis e_{mhe} is reduced from 13% (without hysteresis compensation) to less than 3% (with the WIHC approach). Figure 9(b) shows the trajectory tracking response, and the tracking error is also shown in figure 9(c). The experimental results demonstrate that, with the WIHC approach, e_m and e_{rms} are 2.87% and 0.76%, respectively.

4.3.4. DIHC. Finally, the same test is conducted with the DIHC approach. Figure 10 shows the experimental results. The relationship between the desired position and the actual position is illustrated in figure 10(a). We determine that the DIHC reduces the hysteresis-caused error e_{mhe} from 13% to about 2.5%. The response of the PCA shown in figure 10(b) also verifies the effectiveness of the hysteresis compensation.

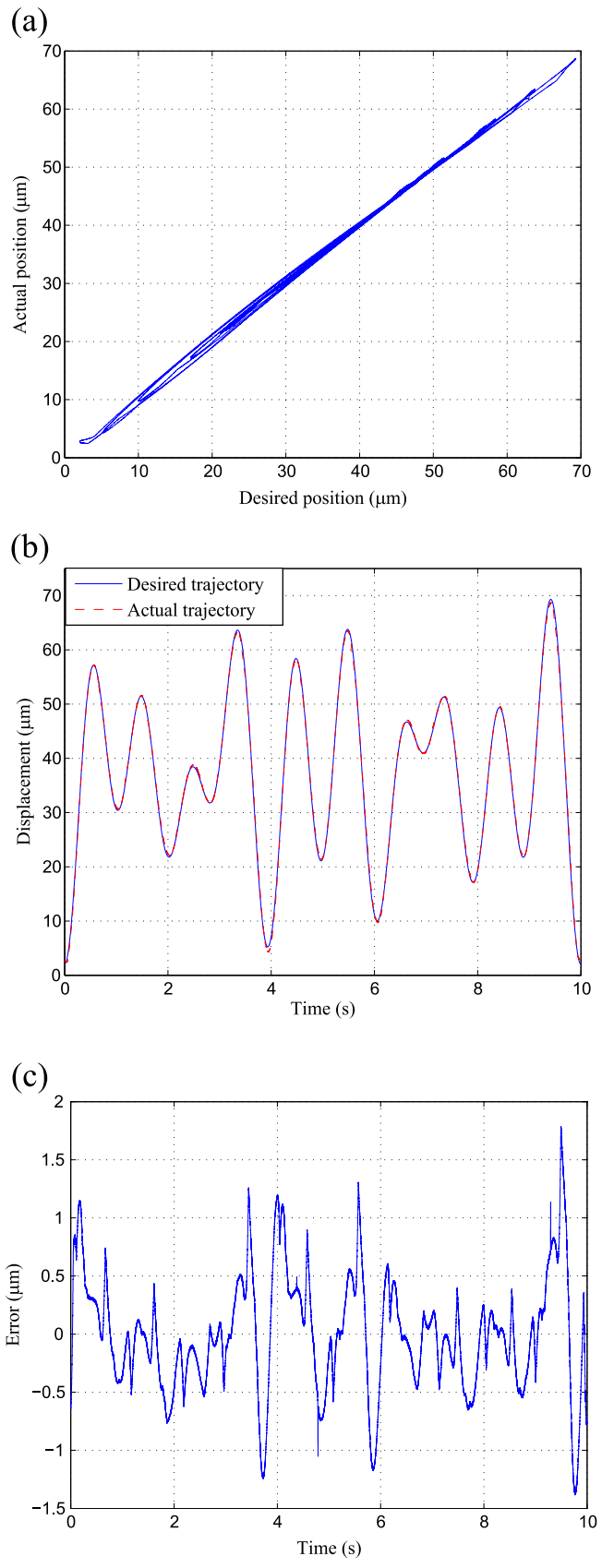

Figure 8. Experimental results with the IHC approach. (a) Relationship of desired and actual position. (b) Response of the PCA (blue solid line: desired trajectory; red dash line: actual trajectory) and (c) Tracking error.

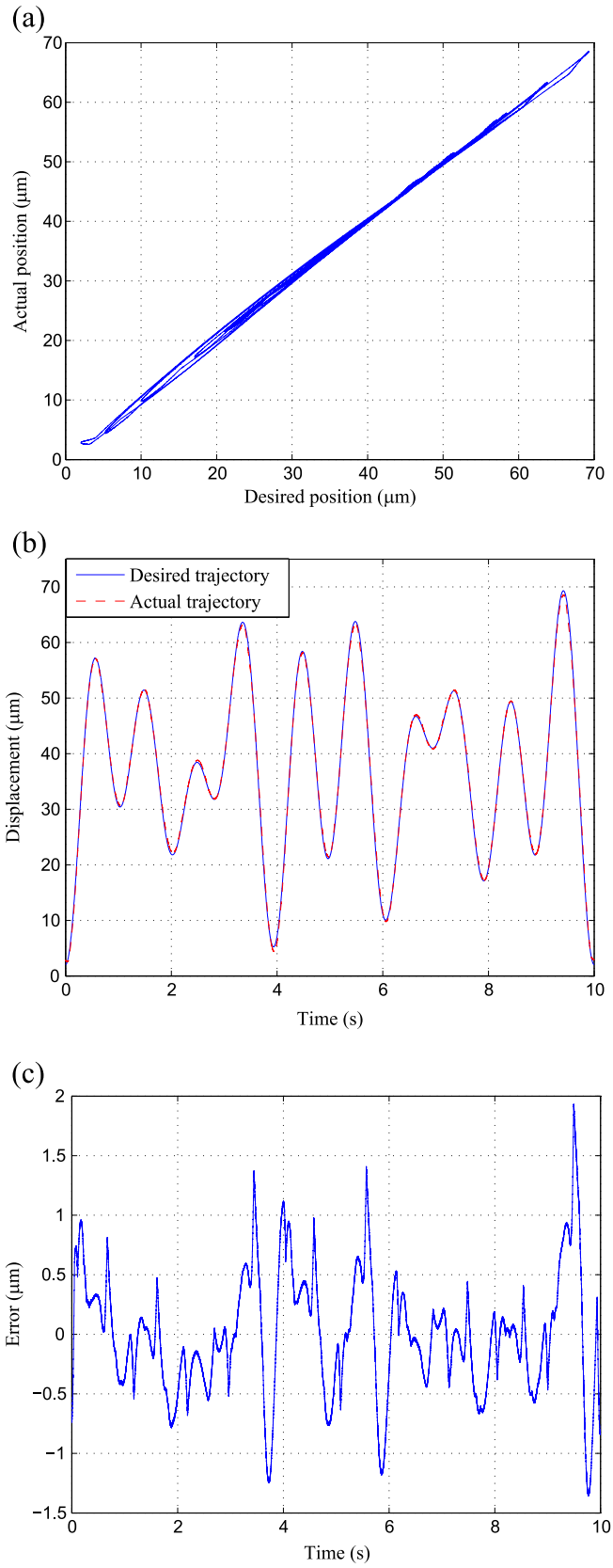

Figure 9. Experimental results with the WIHC approach. (a) Relationship of desired and actual position. (b) Response of the PCA (blue solid line: desired trajectory; red dash line: actual trajectory) and (c) Tracking error.

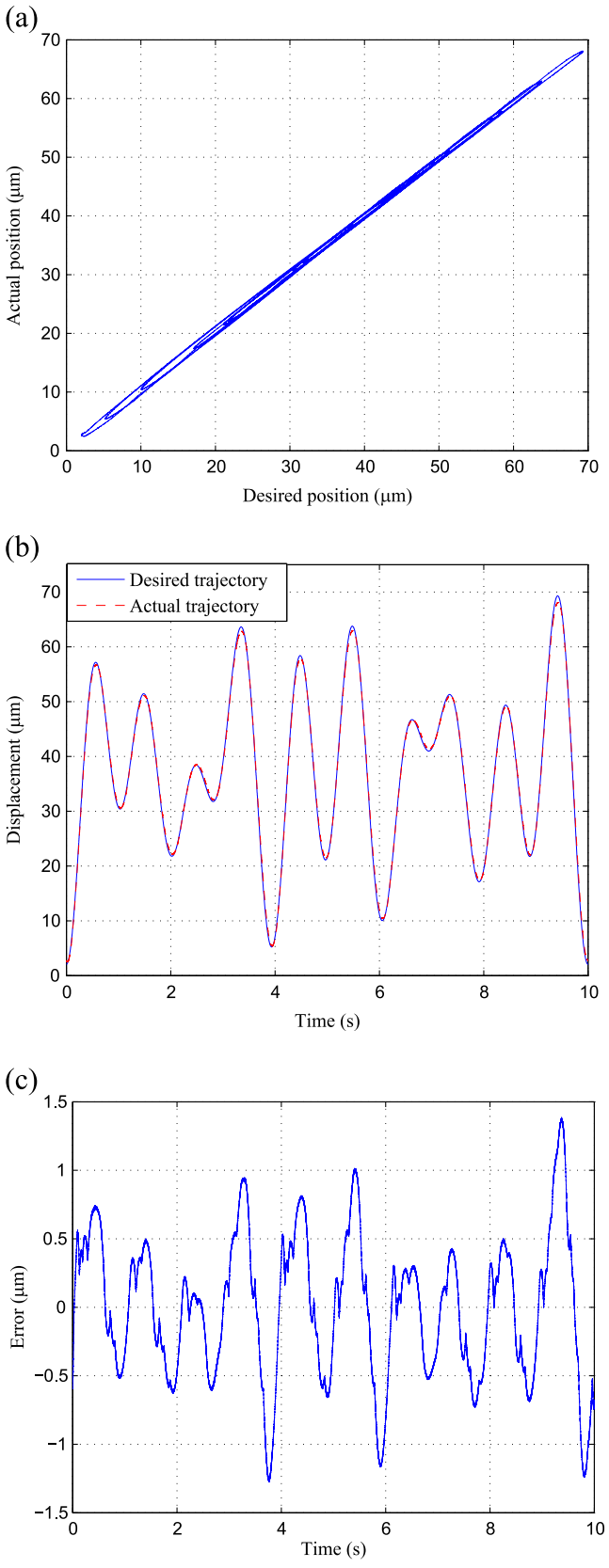

Figure 10. Experimental results with the DIHC approach. (a) Relation of desired and actual position. (b) Response of the PCA (blue solid line: desired trajectory; red dash line: actual trajectory) and (c) Tracking error.

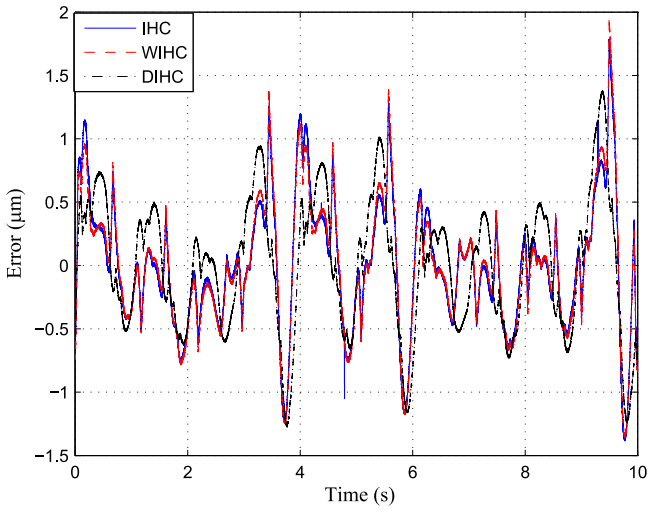

Figure 11. Comparison of the tracking errors with the three approaches.

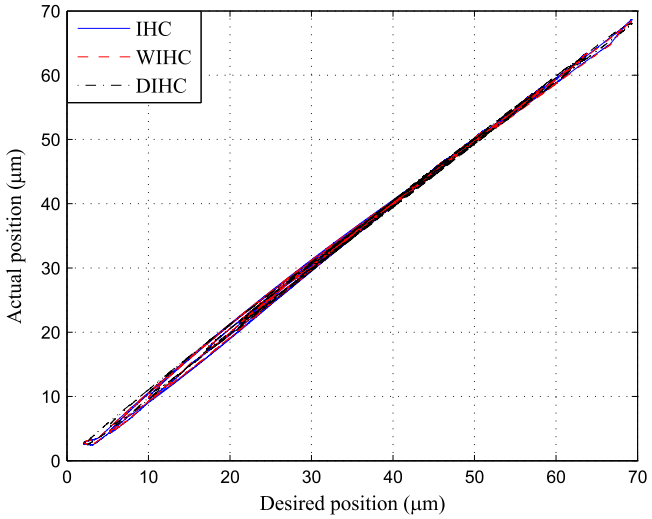

Figure 12. Comparison of the results hysteresis with the three approaches.

Table 3. Performance comparison of three approaches.

Index	IHC	WIHC	DIHC
e_{mhe}	3%	3%	2.5%
e_m	2.66%	2.87%	2.06%
e_{rms}	0.75%	0.76%	0.78%

figure 10(c) shows the tracking error with the DIHC. It is determined that e_m and e_{rms} are 2.06% and 0.78%, respectively.

4.3.5. Discussions. As shown in figures 8–10, the experimental results with the IHC, WIHC, and DIHC approaches are presented and analyzed. The three approaches greatly reduce the hysteresis nonlinearity of the PCA. To reflect the hysteresis compensation performance, figures 11 and 12 also show the comparisons of the tracking errors and resulting hysteresis with the three compensation approaches. For a quantified comparison, table 3 summarizes the e_{mhe}, e_m, and e_{rms} with the different approaches. Overall, the performance is rather similar among the three approaches, and the DIHC is superior by the narrowest of margins. Therefore, we can conclude that the IHC, WIHC, and DIHC approaches are all effective for improving hysteresis compensation and tracking accuracy. The main differences among them are due to the specific principles and implementation steps of each approach. Any of them can be adopted in applications with PCAs as designers find convenient.

5. Conclusion

Three feedforward control approaches for hysteresis compensation have been discussed, experimentally verified, and compared in this work. Investigated approaches are the IHC, WIHC, and DIHC with the MPIM. Based on the discussions in the foregoing sections, it is worth mentioning that the IHC approach is the most widely used to compensate for hysteresis. In this approach, the inverse functions of the hysteresis models are required to be constructed for the development of feedforward controllers. In contrast with the IHC approach, which uses inverse models for controller design, the WIHC approach directly utilizes the hysteresis models to develop the feedforward controllers. Thus, the WIHC approach avoids the complicated procedure for constructing inverse functions of the hysteresis models. However, the multiplicative structure is required for developing feedforward compensators in this approach, which may not be applicable to some other hysteresis models, such as the Jiles-Atherton model and the Krasnosel'skii-Pokrovskii model. Based on the fact that the inversion of the hysteresis effect is by nature hysteresis loops, the DIHC approach directly utilizes the hysteresis models to characterize the inverse hysteresis effect of PCAs, which is different from the IHC and WIHC approaches that model the hysteresis effect of PCAs. Hence, the DIHC approach also avoids the construction of the inverse mathematical model and avoids the utilization of the multiplicative structure. From the comparative experimental results with the three approaches, it can be seen that the performance is rather similar among the three approaches, and the DIHC is superior by the narrowest of margins. Therefore, the IHC, WIHC, and DIHC approaches are all effective for improving hysteresis compensation and tracking accuracy. The main differences among them are due to the specific implementation of each approach.

Acknowledgments

This work was in part supported by the National Natural Science Foundation of China under Grant No. 91023047, China Postdoctoral Science Foundation funded project under Grant No. 2014T70415, and Specialized Research Fund for the Doctoral Program of Higher Education under Grant No. 20130073110037

References

[1] Gozen B A and Ozdoganlar O B 2012 Design and evaluation of a mechanical nanomanufacturing system for nanomilling *Precision Engineering* **36** 19–30

[2] Tang H and Li Y 2014 Development and active disturbance rejection control of a compliant micro/nano-positioning piezo-stage with dual-mode *IEEE Trans. Indust. Electron.* **61** 1475–92

[3] Kim H, Kim J, Ahn D and Gweon D 2013 Development of a nano-precision 3-dof vertical positioning system with a flexure hinge *IEEE Transactions on Nanotechnology* **12** 234–45

[4] Yong Y K, Moheimani S O R, Kenton B J and Leang K K 2012 Invited review article: High-speed flexure-guided nanopositioning: Mechanical design and control issues *Rev. Sci. Instrum.* **83** 121101

[5] Habibullah H, Pota H R, Petersen I R and Rana M S 2013 Creep, hysteresis, and cross-coupling reduction in the high-precision positioning of the piezoelectric scanner stage of an atomic force microscope *IEEE Transactions on Nanotechnology* **12** 1125–34

[6] Tuma T, Sebastian A, Lygeros J and Pantazi A 2013 The four pillars of nanopositioning for scanning probe microscopy: The position sensor, the scanning device, the feedback controller, and the reference trajectory *IEEE Control Systems Magazine* **33** 68–85

[7] Devasia S, Eleftheriou E and Moheimani S O R 2007 A survey of control issues in nanopositioning *IEEE Transactions on Control Systems Technology* **15** 802–23

[8] Kuhnen K and Krejci P 2009 Compensation of complex hysteresis and creep effects in piezoelectrically actuated systems-A new Preisach modeling approach *IEEE Transactions on Automatic Control* **54** 537–50

[9] Gu G Y, Zhu L M and Su C Y 2014 Modeling and compensation of asymmetric hysteresis nonlinearity for piezoceramic actuators with a modified Prandtl-Ishlinskii model *IEEE Trans. Indust. Electron.* **61** 1583–95

[10] Fleming A J and Leang K K 2008 Charge drives for scanning probe microscope positioning stages *Ultramicroscopy* **108** 1551–7

[11] Bazghaleh M, Grainger S, Mohammadzaheri M, Cazzolato B and Lu T F 2013 A digital charge amplifier for hysteresis elimination in piezoelectric actuators *Smart Mater. Struct.* **22** 075016

[12] Okazaki Y 1990 A micro-positioning tool post using a piezoelectric actuator for diamond turning machines *Precision Engineering* **12** 151–6

[13] Sebastian A and Salapaka S 2005 Design methodologies for robust nano-positioning *IEEE Transactions on Control Systems Technology* **13** 868–76

[14] Tsai M S, You S H and Jeng J T 2011 Robust control of a high-precision positioning stage using an integrated h and qft controller *Journal of Intelligent Material Systems and Structures* **22** 421–33

[15] Xu Q 2014 Digital sliding mode control of piezoelectric micropositioning system based on input-output model *IEEE Trans. Indust. Electron.* **61** 5517–26

[16] Liaw H C and Shirinzadeh B 2011 Robust adaptive constrained motion tracking control of piezo-actuated flexure-based mechanisms for micro/nano manipulation *IEEE Trans. Indust. Electron.* **58** 1406–15

[17] Wen C and Cheng M 2013 Development of a recurrent fuzzy cmac with adjustable input space quantization and self-tuning learning rate for control of a dual-axis piezoelectric actuated micro motion stage *IEEE Trans. Indust. Electron.* **60** 5105–15

[18] Ge P and Jouaneh M 1997 Generalized Preisach model for hysteresis nonlinearity of piezoceramic actuators *Precision Engineering* **20** 99–111

[19] Leang K K, Zou Q and Devasia S 2009 Feedforward control of piezoactuators in atomic force microscope systems *IEEE Control Systems Magazine* **29** 70–82

[20] Gu G Y, Yang M J and Zhu L M 2012 Real-time inverse hysteresis compensation of piezoelectric actuators with a modified Prandtl-Ishlinskii model *Rev. Sci. Instrum.* **83** 065106

[21] Liu S and Su C 2013 A modified generalized prandtl-ishlinskii model and its inverse for hysteresis compensation *American Control Conference* 4759–64

[22] Xiao S and Li Y 2013 Modeling and high dynamic compensating the rate-dependent hysteresis of piezoelectric actuators via a novel modified inverse preisach model *IEEE Transactions on Control Systems Technology* **21** 1549–57

[23] Qin Y, Tian Y, Zhang D, Shirinzadeh B and Fatikow S 2013 A novel direct inverse modeling approach for hysteresis compensation of piezoelectric actuator in feedforward applications *IEEE/ASME Transactions on Mechatronics* **18** 981–9

[24] Li Z, Su C Y and Chai T 2013 Compensation of hysteresis nonlinearity in magnetostrictive actuators with inverse multiplicative structure for preisach model *IEEE Transactions on Automation Science and Engineering* **11** 613–9

[25] Krejci P and Kuhnen K 2001 Inverse control of systems with hysteresis and creep *IEE Proceedings of Control Theory and Applications* **148** 185–92

[26] Ge P and Jouaneh M 1996 Tracking control of a piezoceramic actuator *IEEE Transactions on Control Systems Technology* **4** 209–16

[27] Tan U X, Latt W T, Shee C Y, Riviere C N and Ang W T 2009 Feedforward controller of ill-conditioned hysteresis using singularity-free Prandtl-Ishlinskii model *IEEE/ASME Transactions on Mechatronics* **14** 598–605

[28] Hu H and Mrad R B 2004 A discrete-time compensation algorithm for hysteresis in piezoceramic actuators *Mechanical Systems and Signal Processing* **18** 169–85

[29] Mokaberi B and Requicha A A G 2008 Compensation of scanner creep and hysteresis for AFM nanomanipulation *IEEE Transactions on Automation Science and Engineering* **5** 197–206

[30] Gu G Y, Zhu L M and Su C Y 2014 Integral resonant damping for high-bandwidth control of piezoceramic stack actuators with asymmetric hysteresis nonlinearity *Mechatronics* **24** 367–75

[31] Tan U X, Latt W T, Shee C Y, Riviere C and Ang W T 2007 Modeling and control of piezoelectric actuators for active physiological tremor compensation *Human-Robot Interaction* 1st edn (Vienna: I-Tech)

[32] Wang G, Guan C, Zhou H, Zhang X and Rao C 2013 Hysteresis compensation of piezoelectric actuator for open-loop control *Chinese Optics Letters* **11** S21202

[33] Rakotondrabe M 2011 Bouc-Wen modeling and inverse multiplicative structure to compensate hysteresis nonlinearity in piezoelectric actuators *IEEE Transactions on Automation Science and Engineering* **8** 428–31

[34] Lin C J and Lin P T 2012 Tracking control of a biaxial piezo-actuated positioning stage using generalized duhem model *Computers & Mathematics with Applications* **64** 766–87

[35] Xu Q 2013 Identification and compensation of piezoelectric hysteresis without modeling hysteresis inverse *IEEE Trans. Indust. Electron.* **60** 3927–37

[36] Croft D, Shed G and Devasia S 2001 Creep, hysteresis, and vibration compensation for piezoactuators: atomic force microscopy application *ASME Journal of Dynamic Systems, Measurement, and Control* **123** 35–43

[37] Li W and Chen X 2013 Compensation of hysteresis in piezoelectric actuators without dynamics modeling *Sensors and Actuators A: Physical* **199** 89–97
[38] Fleming A J 2013 A review of nanometer resolution position sensors: operation and performance *Sensors and Actuators A: Physical* **199** 106–26
[39] Yang M J, Gu G Y and Zhu L M 2013 Parameter identification of the generalized Prandtl-Ishlinskii model for piezoelectric actuators using modified particle swarm optimization *Sensors and Actuators A: Physical* **189** 254–65
[40] Truong B N M, Nam D N C and Ahn K K 2013 Hysteresis modeling and identification of a dielectric electro-active polymer actuator using an apso-based nonlinear preisach narx fuzzy model *Smart Mater. Struct.* **22** 095004